EMAS Engineering Modelling, Analysis & Simulation THE NAFEMS JOURNAL

NAFEMS

Vol. 1, Issue 1, 2024

Simulation-based digital twin of a high-speed turbomachine (fan) used in avionics cooling

M. Kandaz[a,1], A. Kaçar[a], U. Gündoğar[a], E. Ak[a], C. Alpdoğan[a]

[a]Numesys Advanced Engineering Co., Turkey

Abstract

In this contribution, the simulation-based digital twin of a high-speed turbomachine, i.e. a fan with a nominal speed of 16500 rpm, that has been developed for the aerospace industry with multiple uses in various platforms, and the corresponding findings are presented. The relevant simulation-based digital twin is created by first running various multi-physics engineering simulations, i.e. computational solid mechanics, computational fluid dynamics, and low-frequency electromagnetic analyses with Ansys software. Subsequent dynamic reduced order models (ROM) are formed and integrated together to create the digital twin that are bidirectionally connected with the asset. The digital twin is also validated via experimental data that are obtained with various setups for several parameters read at discrete locations via sensors, based on fidelity comparisons both between experiments and simulations, and between simulations and ROMs. Several operational scenarios including those with stress tests are run and the asset is checked against fatigue and thermal requirements for the rotor-stator assembly and the motor circuit respectively. This is done with an inhouse program that incrementally reads time, temperature, and rotational speed data and in which the relevant fatigue and thermal criteria are defined. This program is also used to simulate and analyse what-if scenarios. It is seen that vibration fatigue dominates all possible sources of failure in most cases. As a novel aspect, the fatigue induced by starts and stops of the fan is expressed as equivalent operating hours (EOH) depending on time and temperature parameters of the corresponding scenarios, as opposed to be taken as a constant value for all scenarios. Using this novelty, it is also conceptually demonstrated that simulation-based digital twins can play a significant role in operation and maintenance (O&M) when combined with conventional data-driven predictive maintenance techniques, not only for O&M teams but also asset owners and original equipment manufacturers (OEMs) particularly with the use of what-if analyses. Approaches to simulation-based digital twins in context with multi-physics and ROM fidelity are also discussed based on several digital twin maturity models.

Keywords

turbomachinery, digital twins, ROM, multiphysics, failure, condition monitoring, FEA

1 Introduction

Advancing technology, competition, and specialization drives our modern world and products evolve into cyber-physical systems (CPS) with mechanical, electrical, and software components [1]. This ever-growing complexity is further enriched with the inclusion of digital twins based on internet of things (IoT), Industry 4.0, smart systems [2]. There are many definitions of digital twins, but the most general definition can be quoted as “a live digital coupling of the state of a physical asset or process to a virtual representation with a functional output” ([3], [4]). It can also be fundamentally defined as a digital representation of a product or a process (physical twin – PT), synchronized at a certain fidelity and

[1]Corresponding author.
E-mail address: murat.kandaz@numesys.com.tr
https://doi.org/10.59972/0h0r0793

frequency, as a part of a CPS [5]. Digital twins are being used in many industries already, including manufacturing ([6], [7]), energy ([8], [9]), construction [10], aerospace ([11], [12]), and many others, specifically for condition monitoring and predictive maintenance ([13]-[15]).

Together with the conventional data-based approach, simulation-based digital twin technology allows detection of problems that may occur in components, testing existing or new configurations, creating and perform what-if analyses. Embedded in the relevant asset or run in a cloud-based environment, engineering simulation software can model the life cycle of the asset based on engineering physics. Since real-time mimicking of the conditions by the relevant software requires major computer resources, the related operations are performed with reduced order models (ROM).

The aim of this study is to quantitatively identify predictive maintenance metrics and the impact of start and stops of a turbomachine, one of the major type of machines for which digital twins are being studied. Along with the standard mean time to failure (MTTF) metric, another quantity for starts and stops is expressed in terms of the equivalent operating hours (EOH). Starts and stops are assumed to induce fatigue on a machine, as if the machine runs over a time that is equal to EOH, which is an important metric upon which turbomachines' performance characteristics are quantified. OEMs have different numerical representation schemes, but a generic EOH vs performance degradation curve is as given in Figure 1 (performance degradation in efficiency and power of the turbomachine). An avionics cooling fan is selected for this purpose and the simulation-based digital twin is created using engineering simulations.

The study also involves the use of an existing IoT software and platform, along with configuration of this platform's input-output connections to and from sensors-actuators deployed on the fan, as well as development of an inhouse program. However, most of the details of these are left out to focus more on the use of engineering simulations in digital twins. For this purpose, Section 2 includes system modelling and Section 3 contains detailed information about individual simulations. Section 4 concludes the paper with results, remarks, and ideas for future studies.

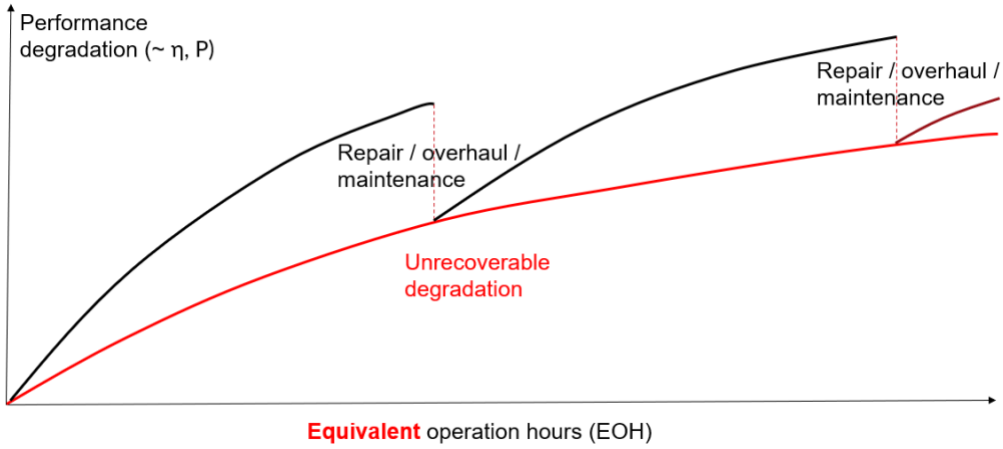

Figure 1. A generic EOH vs performance (degradation) curve.

2 Modelling

The fan is exposed to many extreme and variable loads and conditions throughout its life cycle. High and/or variable fluid velocity, temperature and pressure, structural strains and stresses, electrical losses and thermal effects related to them are the most important ones. Since the effect of starts and stops are of concern, shock loads or reaction forces due to aircraft manoeuvres have not been considered.

As a result of analyses of requirements, experimental setup and geometry limitations of the fan, the variables and physics as depicted in Figure 2 have been included in the scope of the study. Herein each neural network in fact represents the dynamic ROM of the relevant engineering simulation (computational fluid dynamics – CFD, computational solid mechanics – CSM, electromagnetic analyses – EMA), formed by Ansys Twin Builder.

The inputs of the system consist of rotational speed $\boldsymbol{\omega}$, ambient air density $\boldsymbol{\rho}$, ambient air temperature $\boldsymbol{T_0}$, volumetric flow rate $\boldsymbol{Q}$, vibration acceleration $\boldsymbol{a}$. These are also parameters read during operation of the fan and fed into the system to simulate interim parameters as current $\boldsymbol{I}$, voltage $\boldsymbol{V}$, differential

pressure ΔP, air temperature of the fan outlet T_1, and electrical losses $\dot{E}$. There are in turn two output parameters as equivalent stress σ of the stator-rotor assembly that is used for assessing vibration fatigue and temperature difference ΔT of the motor that is used for checking relevant thermal requirements.

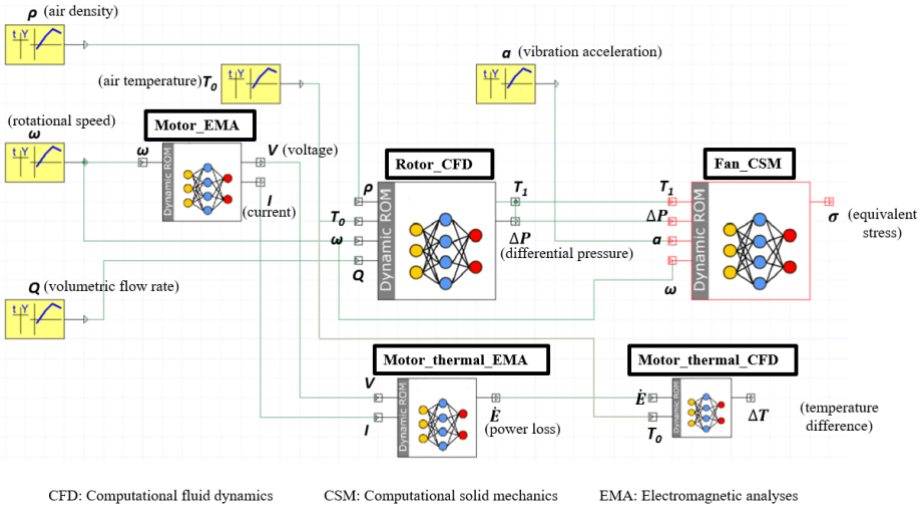

Figure 2. System simulation model indicating the parameters and engineering physics considered in the digital twin.

3 Engineering Simulations

Ansys simulation software, namely Fluent for CFD, Mechanical for CSM, and Maxwell for EMA are selected in line with Ansys Twin Builder. Geometry cleaning before relevant simulations is performed via Ansys SpaceClaim.

The nominal rotational speed of the fan is 16500 rpm which represents the highest speed in a turbomachine of which a digital twin is being created, according to the best knowledge of the authors. Hence the fidelity of the CFD simulation is also of concern. To tackle this issue, the experimental setup that is depicted in Figure 3 is made use of. The setup consists of four chambers separated by two perforated plates and a nozzle per the relevant standard [16]. The CFD model of the fan is first created for this setup for various conditions given in Figure 4 and relevant comparisons are made. between simulation results and experimental data, as depicted in Figure 5.

A mesh sensitivity analysis is also performed that yielded a mesh with 10.1 million elements is satisfactory to mimic the behaviour of the fan in almost all flow conditions, with an average compatibility of 95%. This is per arithmetic average of differences of volumetric flow rate values (y-axis of Figure 5) based on different number of differential pressure values (x-axis of Figure 5). The results with different mesh sizes and different data points are as presented in Table 1.

To assess MTTF and EOH metrics based on equivalent stress σ, 1-way CFD and CSM analyses of the rotor are performed. For CFD side the fan is modelled on its operating environment based on different boundary conditions for rotational speed ω, ambient air density ρ, ambient air temperature T_0, volumetric flow rate Q. The relevant parameter set is given in Table 2. All the variations correspond to 1485 different combinations of boundary conditions, for which differential pressure ΔP and air temperature of the fan outlet T_1 are found and passed on to CSM analyses. Pressure contours for one of the combinations are as depicted in Figure 6.

CSM analyses for the fan include the addition of vibration acceleration a. Since every imbalance induced by many factors (crack, mass imbalance, deformation, and so on) can lead to vibration and such imbalances are very hard to detect or simulate for every possible combination, vibration acceleration is imposed as a generic boundary condition on horizontal x-axis of the fan. Relevant values and dynamic responses are based on both experimental findings and operational expectations, as given in Table 3. The addition of five different parameters for the vibration acceleration with the previous 1485 combinations hence lead to 7425 different combinations for equivalent stresses σ.

To assess failure condition caused by vibration fatigue, the CSM analyses are performed with power spectral density (PSD) method for vibration accelerations and corresponding equivalent stress values are interpreted using the three-band technique using Miner's cumulative damage ratio [17]. Herein the vibrations induced are formed for start to maximum rotational speed based on experiments. The maximum amplitudes of accelerations are imposed on resonance points. The equivalent stresses are then found for respective standard variations. Equivalent stress corresponding to one standard deviation for a sample combination is as depicted in Figure 7.

To assess failure condition caused by thermal stresses, relevant temperature change requirement recommended by the printed circuit board (PCB) manufacturer is followed, with a separate EMA and CFD analyses workflow as depicted in Figure 2. Herein the most important criterion is defined as the temperature difference ΔT for the motor. The relevant structure of the motor and the driver circuit is depicted in Figure 8 with the corresponding torque and current values and respective response surfaces are given in Figure 9.

After all analyses given in Figure 2 are run at values that are distributed over operation regime and relevant dynamic ROMs are generated, these values are transferred to a program as the "data lake" of the simulation outputs. This program, developed inhouse, then uses the above-mentioned three-band technique and Miner's cumulative damage rule along with the relevant temperature changes, and temperature change gradients. When a certain operation profile is loaded, relevant failure conditions can be checked using the abovementioned techniques and corresponding algorithms, and relevant MTTF values along with the EOH impact of starts and stops can be found, as detailed in Section 4.

Table 1. Average compatibilities between experimental data and simulation results based on mesh size. (Relevant data points on x axis are given in Figure 5.)

Mesh size	3 data points	5 data points	11 data points	21 data points
[10^6]	(x = 25, 150, 275 cfm)	(x = 50, 100, 150, 200, 250 cfm)	(x = 25, 50, … 250, 275 cfm)	(x = 25, 37.5, … 262.5, 275 cfm)
1.1	% 62.1	% 64.5	% 66.4	% 67.5
2.2	% 68.5	% 69.5	% 70.1	% 70.2
3.0	% 78.7	% 79.1	% 80.1	% 80.3
5.8	% 83.6	% 84.1	% 84.3	% 84.5
7.6	% 85.4	% 91.3	% 94.7	% 96.2
10.1	% 88.7	% 93.2	% 95.1	% 96.8
13.2	% 89.0	% 93.4	% 95.3	% 97.1
16.4	% 89.2	% 93.5	% 95.5	% 97.3

Table 2. Parameter set for CFD analyses for the rotor.

Ambient air density, $\boldsymbol{\rho}$ [g/m^3]	Ambient air temperature, $\boldsymbol{T_0}$ [ºC]	Rotational speed, $\boldsymbol{\omega}$ [rpm]	Volumetric flow rate, $\boldsymbol{Q}$ [cfm]
0.985	-55	15600	25
0.945	-40	16050	50
1.005	-25	16500	75
1.065	-10		100
1.125	+5		125
	+20		150
	+35		175
	+50		200
	+70		225
			250
			275

Table 3. Parameter set for CSM analyses for the rotor.

Rotational speed, ω | frequency, f	Max acceleration, a [g]
15600 rpm = 260 Hz	0.05
16050 rpm = 267.5 Hz	0.15
16500 rpm = 275.0 Hz	0.25
	0.50
	1.00

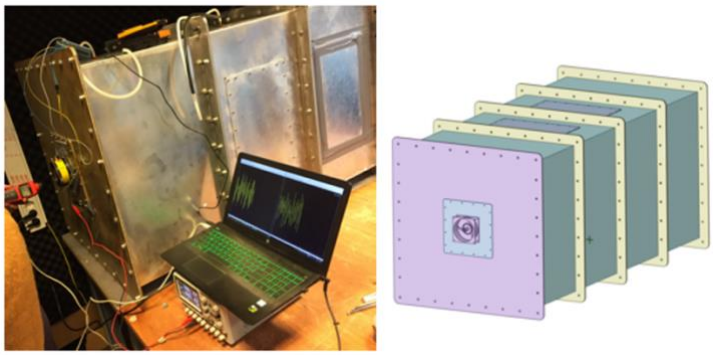

Figure 3. Experimental setup (left) and relevant CAD model (right).

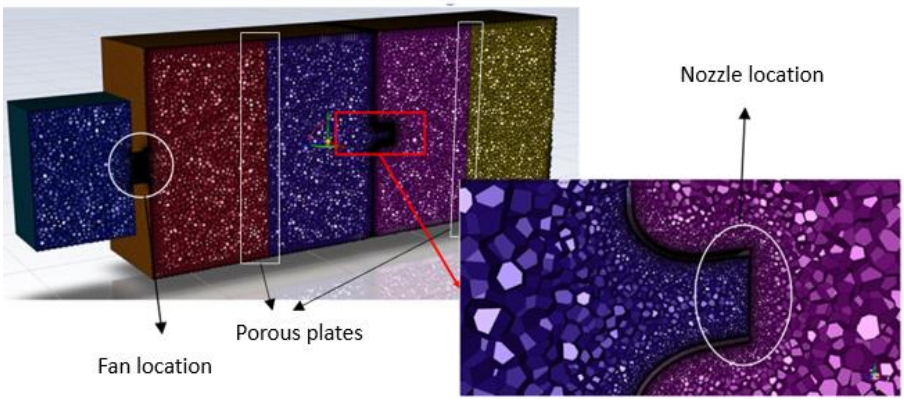

Figure 4. Experimental setup CFD model.

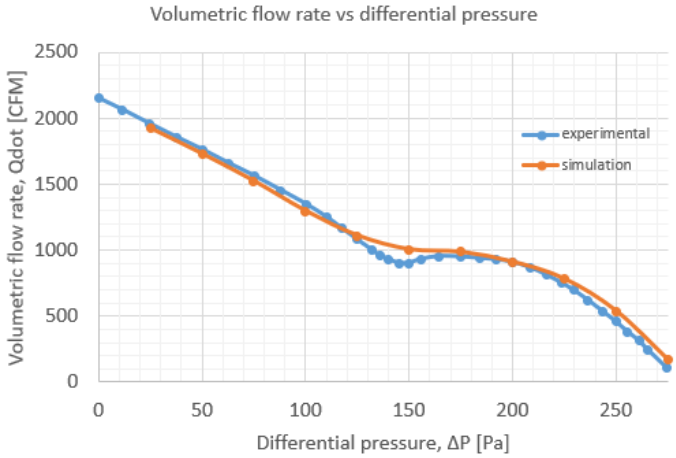

Figure 5. Experimental data vs simulation results for 10.1 million cells.

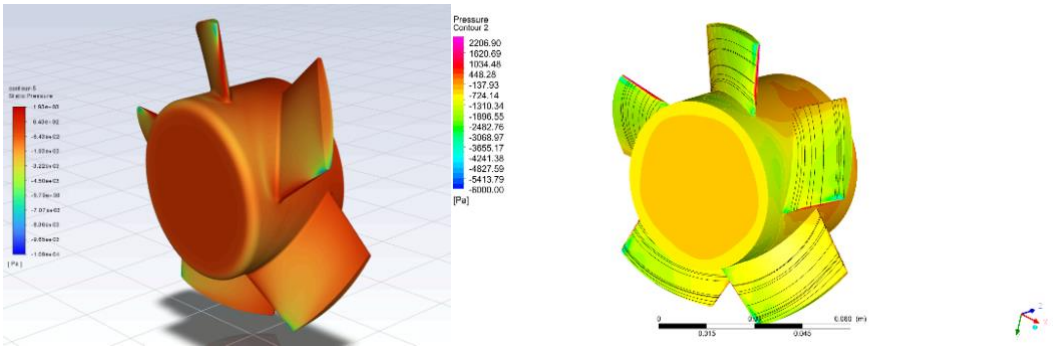

Figure 6. Pressure contours for ρ = 1.005 g/m3, T_0 = 20 ºC, ω = 16500 rpm, Q = 175 cfm.

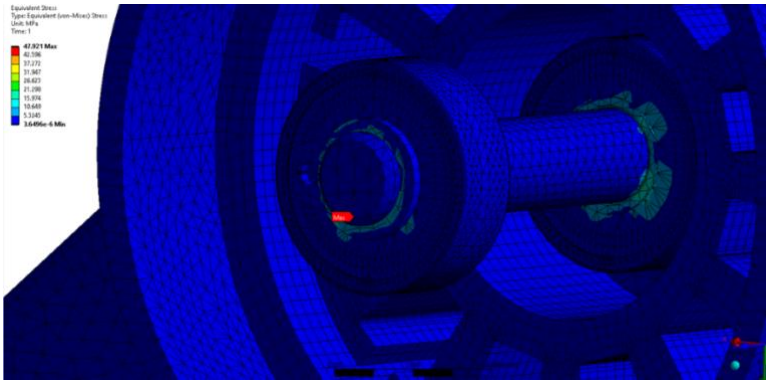

Figure 7. Equivalent stress at one standard deviation for **ρ** = 1.005 g/m3, T_0 = 20 ºC, ω = 16500 rpm, Q = 175 cfm, and **a** = 0.05 g.

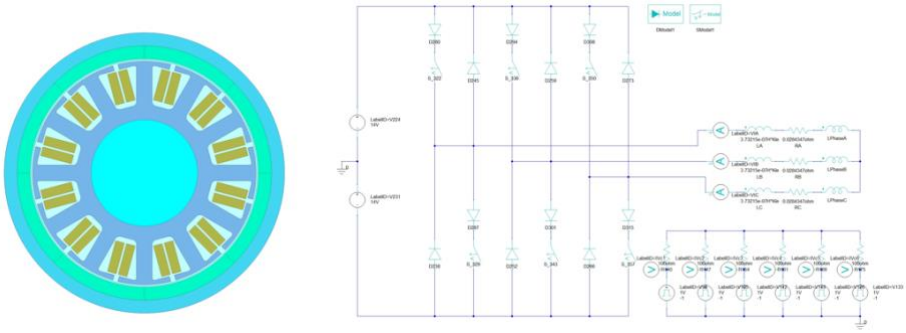

Figure 8. Motor structure (left) and relevant driver circuit model (right).

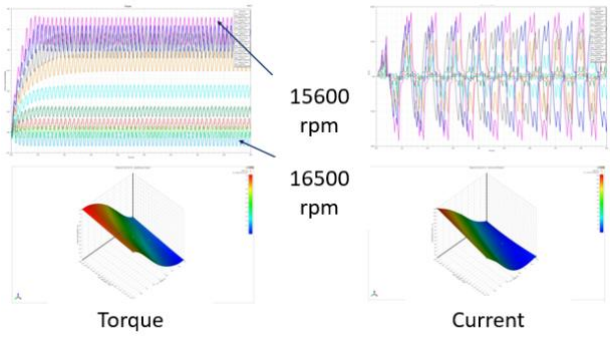

Figure 9. Analysis results for torque (top left) and current (top right) and corresponding response surfaces for torque (bottom left) and current (bottom right).

4 Results and Discussion

To demonstrate numerical results three representative operation scenarios with varying temperature profiles over time are selected as depicted in Figure 10. Herein black vertical lines indicate starts and grey vertical lines indicate stops. The profiles are repeated at the end of the depicted times in minutes. As seen, Scenario 1 contains a relatively regular profile whereas Scenario 3 is filled with starts and stops with higher temperature gradients. The resulting MTTF and average EOH values for all relevant starts and stops are presented in Table 2. As expected, Scenario 3 yields the maximum EOH's and correspondingly the minimum MTTF value, in contrast to those in Scenario 1, where Scenario 2 yields the results in between.

This suggests that, with this concept,

- the effect of starts and stops to fatigue can be quantitatively described, at least relative to each other based on different operation regimes,
- operation and maintenance (O&M) teams can
- foresee overhaul/repair/maintenance periods,
- operate the assets healthier in a more durable fashion based on EOH vs performance curves,
- asset owners and OEMs can also perform what-if analyses for various operation profiles and foresee the overhaul/repair/maintenance periods.

Considering the nature of the use and the reliance on engineering simulations, the place and evolution of the digital twin in respective maturity models is of crucial concern. Using maturity models as a self-assessment tool about the current situation and the future of the digital twin, respective referenced models are studied [18]. In terms of engineering simulations, its effect on various modelling dimensions is best captured in "digital twin 8-dimension model" [1]. Herein the effect of several design elements is also reflected on dimensions that help evaluating the maturity. It is revealed that the digital modelling element consisting of CAD models, CAE models, algebraic models, numerical models, and statistical models are the most important element considering all dimensions. These models also essentially required for integration breadth, CPS intelligence, simulation capabilities, digital model richness, and life cycle.

The engineering analyses for creating the digital twin contain CAD, CAE, and numerical models, whereas ROMs are essentially algebraic models of these simulations. The program developed inhouse also make use of algebraic and statistical models. Hence fidelity should be given attention separately. The fidelity of a digital twin represents the similarity per its physical twin based on both state and behaviour, analyzing the influence of abstraction and resolution [19]. Currently, state-based fidelities for models leading to vibration fatigue prediction given in Figure 2 are found as given in Table 5. Future work involves quantifying fidelity based on behaviour using Needleman-Wunsch (NW) algorithm and to create federated multi-fidelity models based on various conditions. Multi-fidelity models can help regarding the domain of concern (motor, rotor, fan, and so on) and relevant physics. It is then possible to switch between twin models based on the criticality of the equipment.

This study also includes the turbomachine with the highest rotational speed of which a digital twin is studied, according to the best knowledge of the authors. In the future a larger turbomachine with a lower rotational speed (e.g. gas turbine, wind turbine) is aimed to be studied. Since one of the major validation points is in fact the point/time of repair/failure of the equipment, access to O&M data is also going to be a major criterion for future studies.

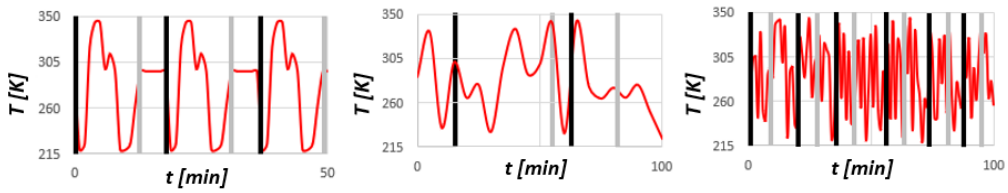

Figure 10. Scenario 1 (left), Scenario 2 (middle), and Scenario 3 (right) as representative operation scenarios (temperature vs time).

Table 4. MTTF and EOH for start and stops for the representative scenarios.

	Scenario 1	Scenario 2	Scenario 3
MTTF	14384	12145	8679
EOH – start	4.2	5.1	6.3
EOH – stop	3.5	3.6	4.1

Table 5. Relevant state-based fidelity values and corresponding approach

Model	Type	Method	Fidelity
Rotor_CFD	Experiment-simulation	Per Table 1	95%
Rotor_CFD	Simulation-ROM	Relative accuracy [20]	95%
Fan_CSM	Experiment-simulation	N/A due to the lack of access to O&M data	N/A
Fan_CSM	Simulation-ROM	Relative accuracy [20]	95%
Motor_EMA	Experiment-simulation	Simulation compared to test values for torque, current, and power	95%
Motor_EMA	Simulation-ROM	Relative accuracy [20]	95%

5 Acknowledgements

The authors gratefully acknowledge the financial support from Turkish Scientific and Technological Research Council (TUBITAK) under grant scheme 1501 with project no 3200874.

6 References

[1] R. Stark, C. Fresemann, and K. Lindow, “Development and operation of Digital Twins for technical systems and services,” *CIRP Annals*, vol. 68, no. 1, pp. 129–132, 2019, doi: 10.1016/j.cirp.2019.04.024.

[2] F. Bordeleau, B. Combemale, R. Eramo, M. van den Brand, and M. Wimmer, “Towards Model-Driven Digital Twin Engineering: Current Opportunities and Future Challenges,” *Communications in Computer and Information Science*, pp. 43–54, 2020, doi: 10.1007/978-3-030-58167-1_4.

[3] H. Boyes and T. Watson, “Digital twins: An analysis framework and open issues,” Computers in Industry, vol. 143, p. 103763, Dec. 2022, doi: https://doi.org/10.1016/j.compind.2022.103763.

[4] H. V. M. Catapult. “Untangling the requirements of a digital twin”. Univ. Sheff. Adv. Manuf. Res. Cent. (AMRC), Oct. 2021.

[5] Glossary,” *Digital Twin Consortium*. https://www.digitaltwinconsortium.org/glossary/glossary/#digital-twin (accessed Sep. 01, 2022).

[6] A. Heininen, R. Prod’hon, H. Mokhtarian, E. Coatanéa, and K. Koskinen, “Finite element modelling of temperature in cylindrical grinding for future integration in a digital twin,” *Procedia CIRP*, vol. 104, pp. 875–880, 2021, doi: 10.1016/j.procir.2021.11.147.

[7] E. P. Hinchy, C. Carcagno, N. P. O’Dowd, and C. T. McCarthy, “Using finite element analysis to develop a digital twin of a manufacturing bending operation,” *Procedia CIRP*, vol. 93, pp. 568–574, 2020, doi: 10.1016/j.procir.2020.03.031.

[8] X. Fang, H. Wang, W. Li, G. Liu, and B. Cai, “Fatigue crack growth prediction method for offshore platform based on digital twin,” *Ocean Engineering*, vol. 244, p. 110320, Jan. 2022, doi: 10.1016/j.oceaneng.2021.110320.

[9] A. K. Sleiti, J. S. Kapat, and L. Vesely, “Digital twin in energy industry: Proposed robust digital twin for power plant and other complex capital-intensive large engineering systems,” *Energy Reports*, vol. 8, pp. 3704–3726, Nov. 2022, doi: 10.1016/j.egyr.2022.02.305.

[10] W. Wang *et al.*, “BIM Information Integration Based VR Modeling in Digital Twins in Industry 5.0,” *Journal of Industrial Information Integration*, vol. 28, p. 100351, Jul. 2022, doi: 10.1016/j.jii.2022.100351.

[11] E. J. Tuegel, A. R. Ingraffea, T. G. Eason, and S. M. Spottswood, “Reengineering Aircraft Structural Life Prediction Using a Digital Twin,” *International Journal of Aerospace Engineering*, vol. 2011, pp. 1–14, 2011, doi: 10.1155/2011/154798.

[12] C. Li, S. Mahadevan, Y. Ling, S. Choze, and L. Wang, “Dynamic Bayesian Network for Aircraft Wing Health Monitoring Digital Twin,” *AIAA Journal*, vol. 55, no. 3, pp. 930–941, Mar. 2017, doi: 10.2514/1.j055201.

[13] J. Wang, L. Ye, R. X. Gao, C. Li, and L. Zhang, “Digital Twin for rotating machinery fault diagnosis in smart manufacturing,” *International Journal of Production Research*, vol. 57, no. 12, pp. 3920–3934, Dec. 2018, doi: 10.1080/00207543.2018.1552032.

[14] M. Liu, S. Fang, H. Dong, and C. Xu, “Review of digital twin about concepts, technologies, and industrial applications,” *Journal of Manufacturing Systems*, Jul. 2020, doi: 10.1016/j.jmsy.2020.06.017.

[15] F. Tao, M. Zhang, Y. Liu, and A. Y. C. Nee, “Digital twin driven prognostics and health management for complex equipment,” *CIRP Annals*, vol. 67, no. 1, pp. 169–172, 2018, doi: 10.1016/j.cirp.2018.04.055.

[16] *ANSI/AMCA 210-16: Laboratory methods of testing fans for certified aerodynamic performance rating*. Air Movement and Control Association International, Inc. and the American Society of Heating, Refrigerating, and Air Conditioning Engineers, 2016.

[17] S. M. Kumar, “Analyzing random vibration fatigue”, *ANSYS Advantage*, vol. II, no. 3, pp. 39-42, 2008.

[18] K. Yong-Woon, “Digital Twin maturity model” 10.13140/RG.2.2.28750.48967, 2020.

[19] P. Muñoz, “Measuring the fidelity of digital twin systems,” *Proceedings of the 25th International Conference on Model Driven Engineering Languages and Systems: Companion Proceedings*, Oct. 2022, doi: 10.1145/3550356.3558516.

[20] ANSYS Twin Builder 2023 R1 Help – Dynamic ROM Builder, Appendix B: ROM Accuracy, Relative (%) Accuracy